

Signature of Parity Anomaly: Crossover from One Half to Integer Quantized Hall Conductance in a Finite Magnetic Field

Huan-Wen Wang,¹ Bo Fu,² and Shun-Qing Shen^{3,*}

¹*School of Physics, University of Electronic Science and Technology of China, Chengdu 611731, China*

²*School of Sciences, Great Bay University, Dongguan 523000, China*

³*Department of Physics, The University of Hong Kong, Pokfulam Road, Hong Kong, China*

The pursuit of understanding parity anomaly in condensed matter systems has led to significant advancements in both theoretical and experimental research in recent years. In this study, we explore the parity anomaly of massless Dirac fermions in a semimagnetic topological insulator (TI) thin film subjected to a finite magnetic field. Our findings reveal an anomalous half-quantized Hall conductance arising from the occupied electronic states far below the Fermi level, which is directly associated with the parity anomaly. This observation demonstrates a crossover from one-half quantized Hall conductance in a metallic phase at zero field to one or zero quantized Hall conductance in the insulating phase at a strong field in the presence of disorders, serving as a key indicator for confirming parity anomaly. Our work provides valuable insights into the intricate relationship between band topology in condensed matter systems and quantum anomaly in quantum field theory.

Introduction Parity anomaly is a conflict between the parity symmetry and U(1) gauge invariance of massless Dirac fermions in quantum field theory [1–5], and exhibits a half-quantized Hall conductance in transport measurements [6–14]. Up to now, several condensed matter systems have been proposed to realize parity anomaly [3, 4, 6]. In his seminal paper [6], Haldane pointed out that massless Dirac fermions occur along the critical line between Chern insulators and trivial insulators. Besides, the massless Dirac fermions are also found on the boundary of three-dimensional TIs [15–23].

Jackiw [8] firstly predicted the one-half quantized Hall conductance of massless Dirac fermions in a continuous model at a finite magnetic field, in which the sign of the Hall conductance depends on whether the zero mode of the Landau levels is filled or not. This prediction was extensively accepted after the observation of quantum Hall effect in graphene, in which the Hall conductance was observed to be $\sigma_{xy} = 2(\nu + 1)\frac{e^2}{h}$ (ν is an integer) [24–26]. Considering the double spin and valley degeneracy, it was reasonably assumed that each Dirac cone contributes $(\nu + \frac{1}{2})\frac{e^2}{h}$ to the Hall conductance [27]. Besides, a strong TI thin film also hosts a pair of the massless Dirac cones of surface fermions [15–19]. For the non-doped case, each Dirac cone is expected to contribute $(\nu + \frac{1}{2})\frac{e^2}{h}$ to the Hall conductance at a finite magnetic field [19, 28–30], which is similar to graphene. By magnetically doping on the one side of a film, or in proximity to a magnetic insulating layer as illustrated in Fig. 1(a), one surface state gap out [31–34], allowing the formation of a single flavor of

massless Dirac fermions on the TI film as schematically shown in Fig. 1(b) [7, 35, 36]. Recently, the measurement of the half-quantized Hall conductance at zero magnetic fields was reported in such a semimagnetic TI [7], and several mechanisms have been proposed [12, 14, 37, 38]. Meanwhile, the conductance flow with decreasing temperatures was shown to converge to the point of $\sigma_{xx} = 0$ or $\sigma_{xy} = \frac{e^2}{h}$ at a magnetic field of 9T, indicating that an integer quantized Hall conductance occurs for a single flavor of massless Dirac fermions at a finite field as shown in Fig. 1(c). This is obviously opposite to Jackiw’s prediction, and inconsistent with experimental observation in graphene and non-magnetic TI films. The flow diagram also shows a qualitatively different pattern to the conventional Hall effect, which causes some confusion in the community [39].

In the present work, we investigate the Hall conductance for a single Dirac cone of the surface fermions in a magnetic field at a semimagnetic TI film by including a time-reversal symmetry breaking term at the higher energy part, which is necessary for the realization of a single flavor of massless Dirac fermions on a lattice. We also demonstrate the evolution of the Hall conductance from one-half at zero fields to zero or one at strong fields in the presence of disorder as indicated by the solid lines in the upper panel of Fig. 1(c). The evolution illustrates that the parity anomaly-related physics occurs for a system with a single flavor of massless Dirac fermions, which is absent in the system with a pair of massless Dirac fermions such as in graphene and TI films. The experimental data [open markers in Fig. 1(c)] extracted from two different and independent experiments on semi-magnetic TIs [7, 35] have already revealed some signatures of parity anomaly in a finite magnetic field. This work clarifies the topological

* sshen@hku.hk

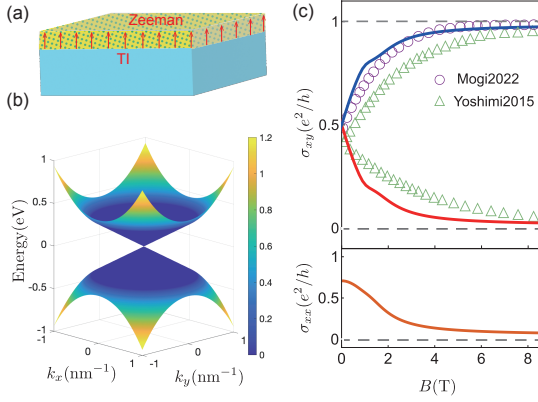


Figure 1. (a) Schematic of a semi-magnetic TI film. (b) The massless Dirac cone in a two-dimensional Brillouin zone, the color represents the relative Dirac mass $m(k^2)/v\hbar k$, in the parity symmetry invariant regime, $m(k^2)/v\hbar k = 0$. (c) The upper panel, crossover from half- to integer-quantized Hall conductance in a finite magnetic field. The open markers are the experimental data extracted from Refs. [7, 35]. The lower panel, longitudinal conductance in a finite magnetic field, which is finite at $B = 0$, and tends to zero in the strong magnetic field. Here the calculation parameters are chosen as $v\hbar = 410 \text{ meV} \cdot \text{nm}$, $b\hbar^2 = -566 \text{ meV} \cdot \text{nm}^2$, $k_c = 0.7 \text{ nm}^{-1}$, $\kappa = 0.001 \text{ nm}^{-2}$.

difference between the systems with a single flavor and two distinct flavors of massless Dirac fermions.

Model Hamiltonian The gapless surface electrons in a three-dimensional TI are usually modeled as ideal Dirac fermions with a linear dispersion [40]. However, when dealing with a single flavor of massless Dirac fermions on a lattice, the inclusion of a time-reversal symmetry broken term in the dispersion becomes inevitable in order to avoid the violation of the fermion doubling theorem [41–43]. Here we start with an effective model for a single massless Dirac cone of the surface states subjected to a perpendicular magnetic field [14]

$$H = \begin{pmatrix} M(\Pi^2) & v(\Pi_x - i\Pi_y) \\ v(\Pi_x + i\Pi_y) & -M(\Pi^2) \end{pmatrix} \quad (1)$$

where the kinematic momentum operator $\Pi_\alpha = -i\hbar\partial_\alpha - eA_\alpha$. The momentum-dependent mass term $M(\Pi^2) = f(k_c^2 - \hbar^2\Pi^2) m(\Pi^2)$, $m(\Pi^2) = -b(\Pi^2 - \hbar^2k_c^2)$ and $f(x) = [1 + \exp(x/\kappa)]$ is the Fermi-Dirac-distribution-like factor with a tiny constant κ . $\hbar k_c$ is a material-specific parameter around which the surface states evolve into the bulk state at a higher momentum part. The model contains the massless linear dispersion at low energy, and also a term that breaks the time-reversal symmetry at higher energy, which is necessary for the existence of a single Dirac cone on a lattice. The linear term

alone does not reflect the anomaly-related physics of the single flavor of massless Dirac fermions[14]. The model can be derived analytically for the surface electrons from a three-dimensional model for TI.

For a uniform magnetic field B along the z -direction, we take the gauge field as $\mathbf{A} = (-By, 0, 0)$. In this case $-i\partial_x$ commutes with the Hamiltonian and can be replaced by its eigenvalues k_x . The ladder operators are introduced as $a = ((y_0 - y)/\ell_B - \ell_B\partial_y)/\sqrt{2}$ and $a^\dagger = [(y_0 - y)/\ell_B + \ell_B\partial_y]/\sqrt{2}$ [44] where the magnetic length $\ell_B = \sqrt{eB/\hbar}$ and the guiding center $y_0 = \hbar k_x/eB$. Then the Hamiltonian is reduced to

$$H = \begin{pmatrix} M[\frac{\hbar^2}{\ell_B^2}(2a^\dagger a + 1)] & \eta a \\ \eta a^\dagger & -M[\frac{\hbar^2}{\ell_B^2}(2a^\dagger a + 1)] \end{pmatrix} \quad (2)$$

with the cyclotron energy $\eta = \sqrt{2}v\hbar/\ell_B$. Take the ansatz for the energy eigenstate $|\psi\rangle = (a_n |n-1\rangle, b_n |n\rangle)^T$ (T represents transpose) and $|n\rangle$ is the eigenket of $a^\dagger a$ with an integer eigenvalue n . The energy eigenvalues are

$$\varepsilon_{ns} = \frac{\omega_n}{2} + s\sqrt{m_n^2 + n\eta^2}, \quad (3)$$

where $\omega_n = M[\frac{\hbar^2}{\ell_B^2}(2n-1)] - M[\frac{\hbar^2}{\ell_B^2}(2n+1)]$ and $m_n = \frac{1}{2} \left\{ M[\frac{\hbar^2}{\ell_B^2}(2n-1)] + M[\frac{\hbar^2}{\ell_B^2}(2n+1)] \right\}$ with $s = \pm$ for $n \geq 1$ and $s = -1$ for $n = 0$. For $n > n_c = b\hbar^2 k_c^2/\omega$, $\varepsilon_{ns} = \frac{\omega}{2} + s\sqrt{(n-n_c)^2\omega^2 + n\eta^2}$ with $\omega = 2b\hbar^2/\ell_B^2$. For $n < n_c$, $\varepsilon_{ns} = s\sqrt{n}\eta$ which are the Landau spectra of massless Dirac fermions [18, 24]. The Landau degeneracy per unit area for each Landau level is $n_L = eB/\hbar$. We have plotted the Landau spectra in the low energy in Fig. 2(a).

Kubo-Streda formula In general, the total Hall conductivity for a two-dimensional electron system can be evaluated by means of the Kubo-Streda formula [45, 46]

$$\sigma_{xy} = \text{Im} \frac{e^2\hbar}{\pi\Omega} \sum_k \int_{-\infty}^{+\infty} n_F(\epsilon - \mu) d\epsilon \times \text{Tr} \left[\hat{v}^x \frac{dG^R}{d\epsilon} \hat{v}^y \text{Im}G^R - \hat{v}^x \text{Im}G^R \hat{v}^y \frac{dG^A}{d\epsilon} \right], \quad (4)$$

where Ω is the area of the two dimensional system, $G^{R/A} = [\epsilon - H \pm i\delta]^{-1}$ is the retarded or advanced Green's function, δ is the disorder-induced band broadening, $\hat{v}^x = i\hbar^{-1}[H, x]$ and $\hat{v}^y = i\hbar^{-1}[H, y]$ are the velocity operators along the x - and y -direction, respectively. $n_F(\epsilon - \mu) = \left[1 + \exp\left(\frac{\epsilon - \mu}{k_B T}\right) \right]^{-1}$ is the Fermi-Dirac distribution function with μ the chemical potential and $k_B T$ the product of Boltzmann

constant and temperature. In this work, we will take advantage of Eq. (4) to study the anomaly-related Hall conductance for both disordered and clean systems.

In the zero magnetic field and clean limit, Eq. (4) leads to the anomalous Hall conductance for massless Dirac fermions as [47]

$$\sigma_{xy}^A = -\frac{e^2}{2h} \left[\text{sgn}(b) + \frac{M(\hbar^2 k_F^2)}{|\mu|} \right],$$

where k_F is the Fermi wave vector and can be found by solving $\mu^2 = v^2 \hbar^2 k_F^2 + M^2(\hbar^2 k_F^2)$. In the parity-symmetry invariant regime, $k_F < k_c$ and $M(\hbar^2 k_F^2) = 0$, the Hall conductance is half-quantized as $\sigma_{xy}^A = -\frac{e^2}{2h} \text{sgn}(b)$, which is only determined by the sign of the quadratic term $m(\Pi^2)$ at higher energy [14]. It can be regarded as a transport signature of parity anomaly in the absence of a magnetic field. For $k_F > k_c$, $M(\hbar^2 k_F^2) \neq 0$, an additional correction makes the Hall conductance deviating from the half-quantized value.

Integer-quantization and parity anomaly To reveal the consequence of the parity anomaly of massless Dirac fermions at a finite magnetic field, we begin with an ideal case of $\delta = 0$. By utilizing the eigenstates and eigenvalues of Eq. (2), we can calculate the retarded and advanced Green's function explicitly. Substituting the calculated Green's functions into the Kubo-Streda formula, one can obtain the Hall conductance at a finite temperature T and chemical potential μ as [47]

$$\sigma_{xy} = -\frac{e^2}{2h} \text{sgn}(b) + \sigma_{xy}^0 \quad (5)$$

with

$$\sigma_{xy}^0 = \frac{e^2}{2h} \left[1 - 2 \sum_{ns} s n_F(s \varepsilon_{ns} - s \mu) \right]$$

where $s = \pm 1$ for $n > 0$ and $s = 1$ for $n = 0$. σ_{xy}^0 has the identical form to the Hall conductance of ideal massless Dirac fermions [27] and is half-quantized as indicated by the green line in Fig. 2. The term $\frac{e^2}{2h}$ in σ_{xy}^0 is caused by the fact that the lowest Landau level of Dirac fermion has twice smaller degeneracy than the levels with $n > 0$. $-\frac{e^2}{2h} \text{sgn}(b)$ in Eq. 5 is an additional contribution from the high energy part as $\lim_{n \rightarrow +\infty} \frac{m_n}{E_n} = -\text{sgn}(b)$ and is a manifestation of parity anomaly. As indicated by the red ($b < 0$) and purple ($b > 0$) solid lines in Fig. 2, the existence of parity anomaly ($-\frac{e^2}{2h} \text{sgn}(b)$) restores the integer-quantization of Hall conductance once the chemical potential is inside the gap of two different Landau levels. From the bulk-edge correspondence, the integer quantum Hall conductance corresponds to the

number of edge states. Moreover, as shown by the gray solid line in Fig. 2(c), the longitudinal conductance σ_{xx} is independent of the b term in the low energy window, and it becomes zero when the Hall conductance is quantized, which makes the measurement more accessible in experiments.

The appearance of $-\frac{e^2}{2h} \text{sgn}(b)$ can also be understood from the spectral asymmetry or Atiyah-Patodi-Singer eta invariant $\eta_H = \sum_{n,s,k_x} \text{sgn}(\varepsilon_{ns})$ [48, 49]. In general, η_H is not convergent and required to be regulated. Here we apply a heat-kernel regularization, i.e., $\eta_H = \lim_{\kappa \rightarrow 0^+} \sum_{k_x, ns} \text{sgn}(\varepsilon_{ns}) e^{-\kappa |\varepsilon_{ns}|}$ [49–51]. As the contribution from ε_{n+} and ε_{n-} is always canceled by each other for a finite n except for $n = 0$, we only need to consider the contribution from a large n . In the case, $\omega_n = \omega$. We can expand the energy spectrum as $\varepsilon_{ns} \approx \frac{\omega}{2} + sn|\omega| + s \text{sgn}(b) \left(\frac{\eta^2}{2\omega} - b \hbar^2 k_c^2 \right)$. Plugging this expression into η_H and making summation over n and s , we have [47]

$$\eta_H = \Omega \frac{eB}{2\pi \hbar} [\text{sgn}(\varepsilon_0) - \text{sgn}(b)]. \quad (6)$$

The first term $\text{sgn}(\varepsilon_0)$ is attributed by the zeroth Landau level ($n = 0$) or low energy, and another term $\text{sgn}(b)$ comes from the part of high energy. For $n = 0$, the energy of the lowest Landau level is either positive or negative depending on the magnetic field and the model parameters, and it naturally contributes to the spectral asymmetry as $\frac{\Omega e B}{2\pi \hbar} \text{sgn}(\varepsilon_0)$. However, for $n > 0$, since there are always two energy levels ε_{n+} and ε_{n-} , one expects that there is no contribution to the spectral symmetry η_H . Hence, the appearance of $\text{sgn}(b)$ in η_H is abnormal, it is a consequence of the parity-symmetry breaking from the electrons of high energy. Furthermore, according to the Streda formula $\sigma_{xy} = -e \frac{\partial \varrho}{\partial B} |_{\mu}$ with $\varrho = -\frac{\eta_H}{2\Omega} + \varrho_0$ the number density of fermions and ϱ_0 the density of charge carriers for empty or filled states relative to the charge neutrality, the spectral asymmetry from the part of high energy corresponds to a half-quantized Hall conductance $-\frac{e^2}{2h} \text{sgn}(b)$. Therefore, the parity-symmetry breaking in the region of high energy indeed leads to a half-quantized Hall conductance.

Crossover from half- to integer-quantization To show the crossover from the half-quantized Hall conductance at a zero field to an integer-quantized Hall conductance at a strong field in Ref. [7], we calculate the Hall conductance in the presence of disorders according to Eq. (4). As displayed by the red line in Fig. 3(a), the Hall conductance is integer-quantized in the clean limit ($\delta \rightarrow 0$), which is consistent with Eq. (5). When δ increases, the peak height of σ_{xy} is suppressed as shown in Fig. 3(a). When δ is strong enough, σ_{xy} exhibits a crossover

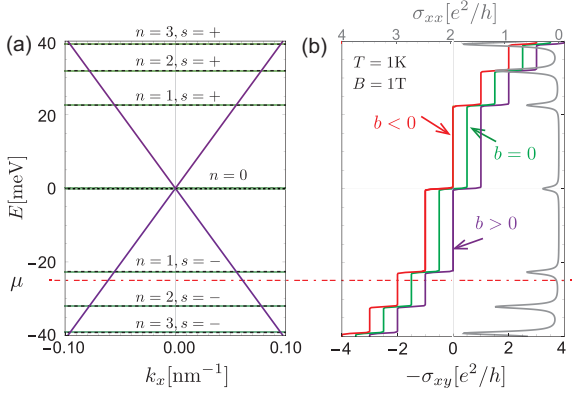


Figure 2. (a) The energy spectrum in the parity symmetry invariant regime. The flat bands are the Landau levels at $B = 1$ T, and the purple line is the energy dispersion in the zero magnetic field. (b) Energy dependence of Hall conductances in Eq. (5) and longitudinal conductance (the gray line) for $b\hbar^2 = -566$ meV \cdot nm², 0 and 566 meV \cdot nm² at $B = 1$ T and $T = 1$ K. The other calculation parameters are chosen as $v\hbar = 410$ meV \cdot nm, $k_c = 0.7$ nm⁻¹, $\kappa = 0.001$ nm⁻². For the longitudinal conductance $\delta = 0.5$ meV.

from one half- to integer-quantization with increasing the magnetic field [purple solid line in Fig. 3(a)]. It should be emphasized that the Hall conductance is always half-quantized in the absence of a magnetic field once the parity symmetry is preserved near the Fermi surface although it is broken as a whole [14]. Hence we have $\sigma_{xy}(0) = -\frac{e^2}{2h} \text{sgn}(b)$ at a finite Fermi energy in Fig. 3(a). In Fig. 3, we put the chemical potential in the valence band ($\mu = -25$ meV), σ_{xy} changes from 0.5 to 1. If we put the chemical potential in the conduction band ($\mu = 25$ meV), as depicted in Fig. 3(b), the crossover will take place between 0.5 and 0, which is in a good agreement with the experiment data by tuning the gate voltage (see Fig. 2b in Ref. [35]). If the chemical potential is comparably even smaller than the band broadening δ , the Hall conductance will deviate from its quantized value. As shown in Fig. 3(b), we tune the chemical potential from -25 meV to 25 meV and fix the band broadening as $\delta = 10$ meV, the Hall conductance at a strong field changes from 1 to 0, and is half-quantized for $\mu = 0$. In experiments, a high-quality sample ($\mu > \delta$) is required to observe the integer-quantized Hall conductance in a finite magnetic field. For instance, as shown in Fig. 3(c), if we set $\delta = |\frac{\mu}{4}|$, the Hall conductance approaches to 1 or 0 for all the chosen chemical potentials except $\mu = 0$. At $\mu = 0$, the Hall conductance is half-quantized as $\sigma_{xy} = -\frac{e^2}{2h} \text{sgn}(b)$, which is robust to the magnetic field, disorder and temperature. Meanwhile, the longitudinal conductivity is also finite at zero tempera-

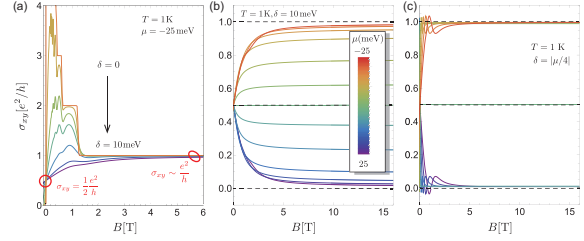


Figure 3. (a) Magnetic field dependence of Hall conductance for massless Dirac fermion with $b\hbar^2 = -566$ meV \cdot nm² for several different band broadenings $\delta = 0, 1, 2, 3, 5, 8, 10$ meV in the parity symmetry invariant regime at $T = 1.0$ K. Here we put the chemical potential at $\mu = -25$ meV [as indicated by the red dashed line in Fig. (2)]. (b-c) Crossover from one half to integer quantized Hall conductance for massless Dirac fermion in the parity symmetry invariant regime. Here we choose the chemical potentials as $\mu = 0, \pm 2, \pm 5, \pm 10, \pm 15, \pm 20, \pm 25$ meV, temperature as $T = 1.0$ K, band broadening as $\delta = 10$ meV in (b) and $\delta = |\mu/4|$ in (c).

ture, $\sigma_{xx}(\mu = 0) = \frac{1}{\pi} \frac{e^2}{h}$ [47]. It is a typical behavior of parity anomalous semimetal in the magnetic field [11].

Impact of particle-hole symmetry breaking In the previous discussion, the Dirac fermions in Eq. (1) preserve the particle-hole symmetry. However, the surface electrons are generally particle-hole asymmetric in TIs. If we further include additional term $-d\Pi^2$ in Eq. (1), the anomalous Hall conductance becomes $\sigma_{xy}^A = -\frac{e^2}{2h} [\text{sgn}(b) + \frac{M(\hbar^2 k_F^2)}{|\mu + d\hbar^2 k_F^2|}]$ at the zero magnetic field. As the additional term is parity symmetry invariant, σ_{xy}^A is still half-quantized for $k^2 < k_c^2$. In a finite magnetic field, the crossover from half- to integer quantization is preserved. In the clean limit, the Hall conductance has an identical form as Eq. (5) by replacing the energy spectra as $\varepsilon_{ns} = -n\omega_D + \frac{\omega_n}{2} + s\sqrt{(\frac{\omega_D}{2} + m_n)^2 + n\eta^2}$ for $n > 0$ and $\varepsilon_0 = -\frac{\omega_D}{2}$ with $\omega_D = \frac{2d\hbar^2}{\ell_B^2}$. Then, the half-quantization of Hall conductance at $\mu = 0$ is destroyed by a magnetic field as the lowest Landau level becomes field-dependent for $d \neq 0$. Nevertheless, the Hall conductance is still half-quantized at $\mu = -\frac{\omega_D}{2}$ and integer-quantized when the chemical potential is inside the gap between two adjacent Landau levels.

Semi-magnetic topological insulator versus graphene Now we come to address the distinctive properties of the Dirac fermions in a semi-magnetic TI and in graphene. There exists a pair of massless Dirac cones in graphene. It does not break the time-reversal symmetry and there is no Hall conductance for each flavor of massless Dirac fermions. Thus, no parity anomaly arises. In this case, two linear Dirac

cones become a good approximation to describe the massless fermions near the Fermi surface. Each Dirac cone has the half-quantized Hall conductance at a finite field according to Jackiw [8]. If we regard the two flavors of massless Dirac fermions share one lowest Landau level, we can obtain the quantized Hall conductance of $(2\nu + 1)e^2/h$ as observed experimentally in graphene [24, 25]. In a semi-magnetic TI, there exists only a single massless Dirac cone as the time-reversal symmetry is already broken by the magnetically doping on one side. The effective Hamiltonian for the massless surface electrons has to include the symmetry-broken term such that it avoids violation of the Nielsen-Nonimiya no-go theorem on a lattice. In other words, without the symmetry-broken term, the model could not reflect the correct physics of a single flavor of massless Dirac fermions on a lattice. With the inclusion of the symmetry broken term, we can see that the Hall conductance is one-half in a metallic phase at a zero field and evolves into one or zero in the insulating phase at a strong field. This resolves the puzzle in Beenakker's commentary on experimental

measurement in the semimagnetic TIs [39].

Summary In short, a crossover from one-half quantized Hall conductance in a metallic phase at a zero field to one or zero quantized Hall conductance in an insulating phase at a strong field in the presence of disorders is a clear signature of parity anomaly of a single flavor of massless Dirac fermions on a lattice. For comparison, in graphene and TI films lacking quantum anomaly, the Hall conductance changes from zero to one quantized Hall conductance for a pair of massless Dirac cones in a magnetic field.

ACKNOWLEDGMENTS

This work was supported by the Research Grants Council, University Grants Committee, Hong Kong under Grant No. C7012-21G and No. 17301823; the Scientific Research Starting Foundation of University of Electronic Science and Technology of China under Grant No. Y030232059002011; and the International Postdoctoral Exchange Fellowship Program under Grant No. YJ20220059.

-
- [1] A. J. Niemi and G. W. Semenoff, Axial-Anomaly-Induced Fermion Fractionization and Effective Gauge-Theory Actions in Odd-Dimensional Space-Times, *Phys. Rev. Lett.* **51**, 2077 (1983).
 - [2] A. N. Redlich, Gauge Noninvariance and Parity Nonconservation of Three-Dimensional Fermions, *Phys. Rev. Lett.* **52**, 18 (1984).
 - [3] G. W. Semenoff, Condensed-Matter Simulation of a Three-Dimensional Anomaly, *Phys. Rev. Lett.* **53**, 2449 (1984).
 - [4] E. Fradkin, E. Dagotto, and D. Boyanovsky, Physical Realization of the Parity Anomaly in Condensed Matter Physics, *Phys. Rev. Lett.* **57**, 2967 (1986).
 - [5] Matthew F. Lapa, Parity anomaly from the Hamiltonian point of view, *Phys. Rev. B* **99**, 235144 (2019).
 - [6] F. D. M. Haldane, Model for a Quantum Hall Effect without Landau Levels: Condensed-Matter Realization of the "Parity Anomaly", *Phys. Rev. Lett.* **61**, 2015 (1988).
 - [7] M. Mogi, Y. Okamura, M. Kawamura, R. Yoshimi, K. Yasuda, A. Tsukazaki, K. S. Takahashi, T. Morimoto, N. Nagaosa, M. Kawasaki, Y. Takahashi, and Y. Tokura, Experimental signature of parity anomaly in semi-magnetic topological insulator, *Nat. Phys.* **18**, 390 (2022).
 - [8] R. Jackiw, Fractional charge and zero modes for planar systems in a magnetic field, *Phys. Rev. D* **29**, 2375 (1984).
 - [9] D. Boyanovsky, R. Blankenbecler, and R. Yahalom, Physical origin of topological mass in 2+ 1 dimensions, *Nucl. Phys. B* **270**, 483 (1986).
 - [10] A. M. J. Schakel, Relativistic quantum Hall effect, *Phys. Rev. D* **43**, 1428 (1991).
 - [11] B. Fu, J. Y. Zou, Z. A. Hu, H. W. Wang, and S. Q. Shen, Quantum anomalous semimetals, *npj Quantum Mater.* **7**, 94 (2022).
 - [12] J. Y. Zou, B. Fu, H. W. Wang, Z. A. Hu, S. Q. Shen, Half-quantized Hall effect and power law decay of edge-current distribution, *Phys. Rev. B* **105**, L201106 (2022).
 - [13] Z. A. Hu, H. W. Wang, B. Fu, J. Y. Zou, and S. Q. Shen, Signature of parity anomaly in the measurement of optical Hall conductivity in quantum anomalous Hall systems, *Phys. Rev. B* **106**, 035149 (2022).
 - [14] J. Y. Zou, R. Chen, B. Fu, H. W. Wang, Z. A. Hu, and S. Q. Shen, Half-quantized Hall effect at the parity-invariant Fermi surface, *Phys. Rev. B* **107**, 125153 (2023).
 - [15] L. Fu, C. L. Kane, and E. J. Mele, Topological Insulators in Three Dimensions, *Phys. Rev. Lett.* **98**.106803 (2007).
 - [16] M. Z. Hasan, and C. L. Kane, Colloquium: Topological insulators, *Rev. Mod. Phys.* **82**, 3045 (2010).
 - [17] X. L. Qi, T. L. Hughes, and S. C. Zhang, Topological field theory of time-reversal invariant insulators. *Phys. Rev. B* **78**, 195424 (2008).
 - [18] S. Q. Shen, *Topological Insulators*, Springer Series of Solid State Science, Vol. 174 (Springer, Heidelberg, 2012).
 - [19] Y. Xu, I. Miotkowski, C. Liu, J. Tian, H. Nam, N. Alidoust, J. Hu, C. K. Shih, M. Z. Hasan, and Y. P. Chen, Observation of topological surface state

- quantum Hall effect in an intrinsic three-dimensional topological insulator, *Nat. Phys.* **10**, 956 (2014).
- [20] R. L. Chu, J. R. Shi, and S. Q. Shen, Surface edge state and half-quantized Hall conductance in topological insulators, *Phys. Rev. B* **84**, 085312 (2011).
- [21] E. J. Koenig, P. M. Ostrovsky, I. V. Protopopov, I. V. Gornyi, I. S. Burmistrov, and A. D. Mirlin, Half-integer quantum Hall effect of disordered Dirac fermions at a topological insulator surface, *Phys. Rev. B* **90**, 165435 (2014).
- [22] S. Zhang, L. Pi, R. Wang, G. Yu, X. -C. Pan, Z. Wei, J. Zhang, C. Xi, Z. Bai, F. Fei, M. Wang, J. Liao, Y. Li, X. Wang, F. Song, Y. Zhang, B. Wang, D. Xing and G. Wang, Anomalous quantization trajectory and parity anomaly in Co cluster decorated BiSbTeSe₂ nanodevices, *Nat. Commun.* **8**, 977 (2017).
- [23] C. Z. Chang, C.-X. Liu, and A. H. MacDonald, Colloquium: Quantum anomalous Hall effect. *Rev. Mod. Phys.* **95**, 011002(2023).
- [24] K. S. Novoselov, A. K. Geim, S. V. Morozov, D. Jiang, M. I. Katsnelson, I. V. Grigorieva, S. V. Dubonos, and A. A. Firsov, Two-dimensional gas of massless Dirac fermions in graphene, *Nature* **438**, 197 (2005).
- [25] Y. B. Zhang, Y. W. Tan, H. L. Stormer, and P. Kim, Experimental observation of the quantum Hall effect and Berry's phase in graphene, *Nature* **438**, 201 (2005).
- [26] A. H. Castro Neto, F. Guinea, N. M. R. Peres, K. S. Novoselov, and A. K. Geim, The electronic properties of graphene, *Rev. Mod. Phys.* **81**, 109 (2009).
- [27] V. P. Gusynin and S. G. Sharapov, Unconventional Integer Quantum Hall Effect in Graphene, *Phys. Rev. Lett.* **95**, 146801(2005).
- [28] R. Yoshimi, A. Tsukazaki, Y. Kozuka, J. Falson, K. S. Takahashi, J. G. Checkelsky, N. Nagaosa, M. Kawasaki, and Y. Tokura, Quantum Hall effect on top and bottom surface states of topological insulator (Bi_{1-x}Sb_x)₂Te₃ films, *Nat. Commun.* **6**, 6627 (2015).
- [29] C. Li, B. de Ronde, A. Nikitin, Y. Huang, M. S. Golden, A. de Visser, and A. Brinkman, Interaction between counter-propagating quantum hall edge channels in the 3D topological insulator BiSbTeSe₂, *Phys. Rev. B* **96**, 195427 (2017).
- [30] S. K. Chong, K. B. Han, T. D. Sparks, and V. V. Deshpande, Tunable Coupling between Surface States of a Three-Dimensional Topological Insulator in the Quantum Hall Regime, *Phys. Rev. Lett.* **123**, 036804 (2019).
- [31] Y. Tokura, K. Yasuda, and A. Tsukazaki, Magnetic topological insulators. *Nat. Rev. Phys.* **1**, 126 (2019).
- [32] Q. Liu, C. X. Liu, C. Xu, X. L. Qi, and S. C. Zhang, Magnetic Impurities on the Surface of a Topological Insulator, *Phys. Rev. Lett.* **102**, 156603 (2009).
- [33] Y. L. Chen, J. H. Chu, J. G. Analytis, Z. K. Liu, K. Igarashi, H. H. Kuo, X. L. Qi, S. K. Mo, R. G. Moore, D. H. Lu, M. Hashimoto, T. Sasagawa, S. C. Zhang, I. R. Fisher, Z. Hussain, and Z. X. Shen, Massive Dirac fermion on the surface of a magnetically doped topological insulator, *Science* **329**, 659 (2010).
- [34] C. Z. Chang, J. Zhang, X. Feng, J. Shen, Z. Zhang, M. Guo, K. Li, Y. Ou, P. Wei, L. L. Wang, Z. Q. Ji, Y. Feng, S. Ji, X. Chen, J. Jia, X. Dai, Z. Fang, S. C. Zhang, K. He, Y. Wang, L. Lu, X. C. Ma, and Q. K. Xue, Experimental observation of the quantum anomalous Hall effect in a magnetic topological insulator, *Science* **340**, 167–170 (2013).
- [35] R. Yoshimi, K. Yasuda, A. Tsukazaki, K. S. Takahashi, N. Nagaosa, M. Kawasaki and Y. Tokura, Quantum Hall states stabilized in semi-magnetic bilayers of topological insulators, *Nat. Commun.* **6**, 8530 (2015).
- [36] R. Lu, H. Sun, S. Kumar, Y. Wang, M. Gu, M. Zeng, Y.-J. Hao, J. Li, J. Shao, X.-M. Ma et al., Half-Magnetic Topological Insulator with Magnetization-Induced Dirac Gap at a Selected Surface, *Phys. Rev. X* **11**, 011039 (2021).
- [37] H. Zhou, H. Li, D. H. Xu, C. Z. Chen, Q. F. Sun, X. C. Xie, Transport Theory of Half-Quantized Hall Conductance in a Semimagnetic Topological Insulator, *Phys. Rev. Lett.* **129**, 096601 (2022).
- [38] M. Gong, H. Liu, H. Jiang, C. Z. Chen, X. C. Xie, Half-Quantized Helical Hinge Currents in Axion Insulators, *Natl. Sci. Rev.* nwad025 (2023).
- [39] C. Beenakker, Anomalous quantum anomalous Hall effect, *J. Club Cond. Matter* October 02 (2022). <https://www.condmatjclub.org/?p=4688>
- [40] W. Y. Shan, H. Z. Lu and S. Q. Shen, Effective continuous model for surface states and thin films of three-dimensional topological insulators, *New J. Phys.* **12**, 043048 (2010).
- [41] H. B. Nielsen and M. Ninomiya, A no-go theorem for regularizing chiral fermions, *Phys. Lett. B* **105**, 219 (1981).
- [42] K. G. Wilson, *New Phenomena in Subnuclear Physics*, ed. A. Zichichi (New York, Plenum, 1975).
- [43] H. J. Rothe, *Lattice gauge theories: an introduction*, 3rd ed. (World Scientific, Singapore, 2005).
- [44] S. Q. Shen, Y. J. Bao, M. Ma, X. C. Xie, and F. C. Zhang, Resonant spin Hall conductance in quantum Hall systems lacking bulk and structural inversion symmetry, *Phys. Rev. B* **71**, 155316 (2005).
- [45] P. Streda, Quantised Hall effect in a two-dimensional periodic potential, *J. Phys. C: Solid State Phys.* **15**, L1299 (1982).
- [46] H. W. Wang, B. Fu, and S. Q. Shen, Intrinsic magnetoresistance in three-dimensional Dirac materials with low carrier density, *Phys. Rev. B* **98**, 081202(R) (2018).
- [47] See Supplemental Material at [URL to be added by publisher] for details of (Sec. S1) Hall conductance in the zero magnetic field, (Sec. S2) Hall conductance in the finite magnetic field, (Sec. S3) longitudinal conductance, and (Sec. S4) calculation of spectral asymmetry η_H , which includes Refs. [44–46, 49, 50].
- [48] M. F. Atiyah, V. K. Patodi, and I. M. Singer, in *Mathematical Proceedings of the Cambridge Philosophical Society* (Cambridge University, Cambridge, England, 1975), Vol. **77**, pp. 43–69.

- [49] A. J. Niemi, Topological solitons in a hot and dense fermi gas, Nucl. Phys. B **251**, 155 (1985).
- [50] J. Böttcher, C. Tutschku, L. W. Molenkamp, and E. M. Hankiewicz, Survival of the Quantum Anomalous Hall Effect in Orbital Magnetic Fields as a Consequence of the Parity Anomaly, Phys. Rev. Lett. **123**, 226602 (2019).
- [51] J. Böttcher, C. Tutschku, and E. M. Hankiewicz, Fate of quantum anomalous Hall effect in the presence of external magnetic fields and particle-hole asymmetry, Phys. Rev. B **101**, 195433 (2020).